Supported by the
U.S. Department of Energy Office of Science
Fusion Energy Sciences

Stability, Transport, and Active MHD Mode Control Analysis of KSTAR High Performance Plasmas Supporting Disruption Avoidance*

Y.S. Park[1], S.A. Sabbagh[1], J.H. Ahn[1], J.W. Berkery[1], Y. Jiang[1], B.H. Park[2], J. Kim[2], H.S. Han[2], S.H. Hahn[2], J.G. Bak[2], J.M. Bialek[1], Y.M. Jeon[2], W.H. Ko[2], M.J. Choi[2], J.S. Ko[2], H.S. Kim[2], H.H. Lee[2], J.H. Lee[2], L. Terzolo[2], S.J. Wang[2], J.G. Kwak[2], S.W. Yoon[2], J.D. Riquezes[1], S. Scott[3], Y.K. In[4], Z. Wang[3], J.-K. Park[3], N.M. Ferraro[3], S.C. Jardin[3], F. Poli[3], M.D. Boyer[3], A.H. Glasser[5], H.K. Park[4], G.S. Yun[6]

[1]Department of Applied Physics, Columbia University, New York, NY, USA
[2]National Fusion Research Institute, Daejeon, Korea
[3]Princeton Plasma Physics Laboratory, Princeton, NJ, USA
[4]UNIST, Ulsan, Korea
[5]Fusion Theory and Computation, Inc., Kingston, WA, USA
[6]POSTECH, Pohang, Korea

presented at the
27th IAEA Fusion Energy Conference
October 22nd – 27th, 2018
Gandhinagar, India

National Fusion Research Institute

COLUMBIA UNIVERSITY IN THE CITY OF NEW YORK

* Work supported by the U.S. Department of Energy under contract DE-FG02-99ER54524 and DE-SC0016614

Abstract of paper EX/P7-16

H-mode plasma operation in KSTAR has surpassed the n = 1 ideal MHD no-wall beta limit computed to occur at β_N = 2.5 with l_i = 0.7. High β_N operation produced β_N of 3.3 sustained for 3 s, limited by tearing instabilities rather than resistive wall modes (RWMs). High fidelity kinetic equilibrium reconstructions (EFIT) have been developed to include Thomson scattering, charge exchange spectroscopy data, and an allowance for fast particle pressure. In addition, motional Stark effect data are used to produce reliable evaluation of the safety factor, q, profile. The reconstructed equilibria can exhibit significant variation of the q-profile dependent upon the broadness of the bootstrap current profile as computed by TRANSP analysis. TRANSP analysis indicates that the non-inductive current fraction can reach up to 75% while its profile can vary significantly depending upon plasma operational scenario. The classical stability of the m/n = 2/1 tearing mode that limited high β_N operation is examined using the resistive DCON code and by the M3D-C^1 code using the kinetic EFIT reconstructions as input. For equilibria at high β_N > 3, the tearing stability index, Δ', is more unstable compared to that of equilibria at reduced β_N. However calculations of instability of stable lower β_N equilibria indicate that the neoclassical components of tearing stability need to be invoked to produce consistency with experiment. MISK code analysis which examines global MHD stability modified by kinetic effects shows significant passive kinetic stabilization of the RWM in these plasmas. Predict-first TRANSP analysis was conducted to design KSTAR plasma operation with 100% non-inductive fraction at β_N above 4. Active RWM control has additionally been enabled on KSTAR. To accurately determine the dominant n-component produced by RWMs expected to onset at higher beta utilizing the new second NBI system, an algorithm has been developed that includes magnetic sensor compensation of the prompt applied field and the field from the induced current on the passive conductors. This analysis on stability, transport, and control provides the required foundation for disruption prediction and avoidance research on KSTAR.

US-KSTAR collaborative research on stability, transport, and active MHD mode control for disruption avoidance

Motivation

- To achieve high performance plasma operation with high non-inductive current fraction without disruptions, the estimation of stability and unique equilibrium and transport properties is crucial
- These analyses will provide the required foundation for disruption prediction and avoidance on KSTAR

S.A. Sabbagh, *et al*., EX/P6-26 in this conference

Outline

- Equilibrium reconstructions using measured kinetic profiles and MSE data for reliable stability and transport analysis
- Transport analysis using TRANSP code to investigate high non-inductive current operation and to optimize the stability
- Ideal and resistive stability analysis using the resistive-DCON, MISK and M3D-C^1 code
- Active RWM feedback algorithm implemented in the KSTAR PCS

KSTAR H-mode equilibria have reached and exceeded the computed n = 1 ideal no-wall stability limit

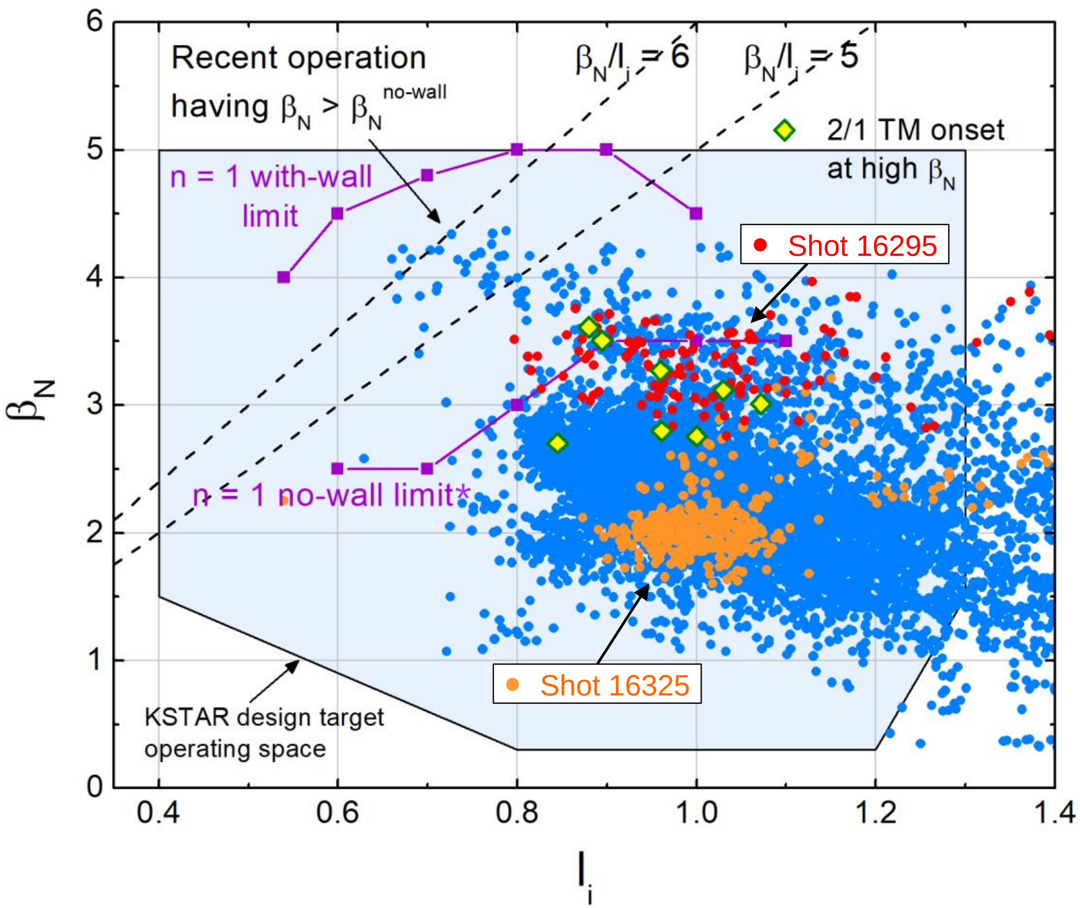

<u>Normalized beta vs. internal inductance from EFIT reconstruction** containing ~9,000 equilibria produced in the 2016 device campaign</u>

*O. Katsuro-Hopkins, *et al.*, Nucl. Fusion **50** (2010) 025019

** Y.S. Park, *et al.*, Nucl. Fusion **53** (2013) 083029

- Parameters for high β_N
  - B_T in range 0.9-1.3 T
  - P_{NBI} = 4.5-5.5 MW
- Highest β_N = 4.3, $\beta_N/l_i > 6$
- MHD stability at high β_N
  - Many equilibria operate above the published ideal n = 1 no-wall stability limit (DCON)
  - Plasma is subject to RWM instability, depending on plasma rotation profile
  - High $\beta_N > \beta_N^{no\text{-}wall}$ operation mostly limited by 2/1 tearing mode onset

High β_N > 3 equilibria limited by MHD - shot 16295

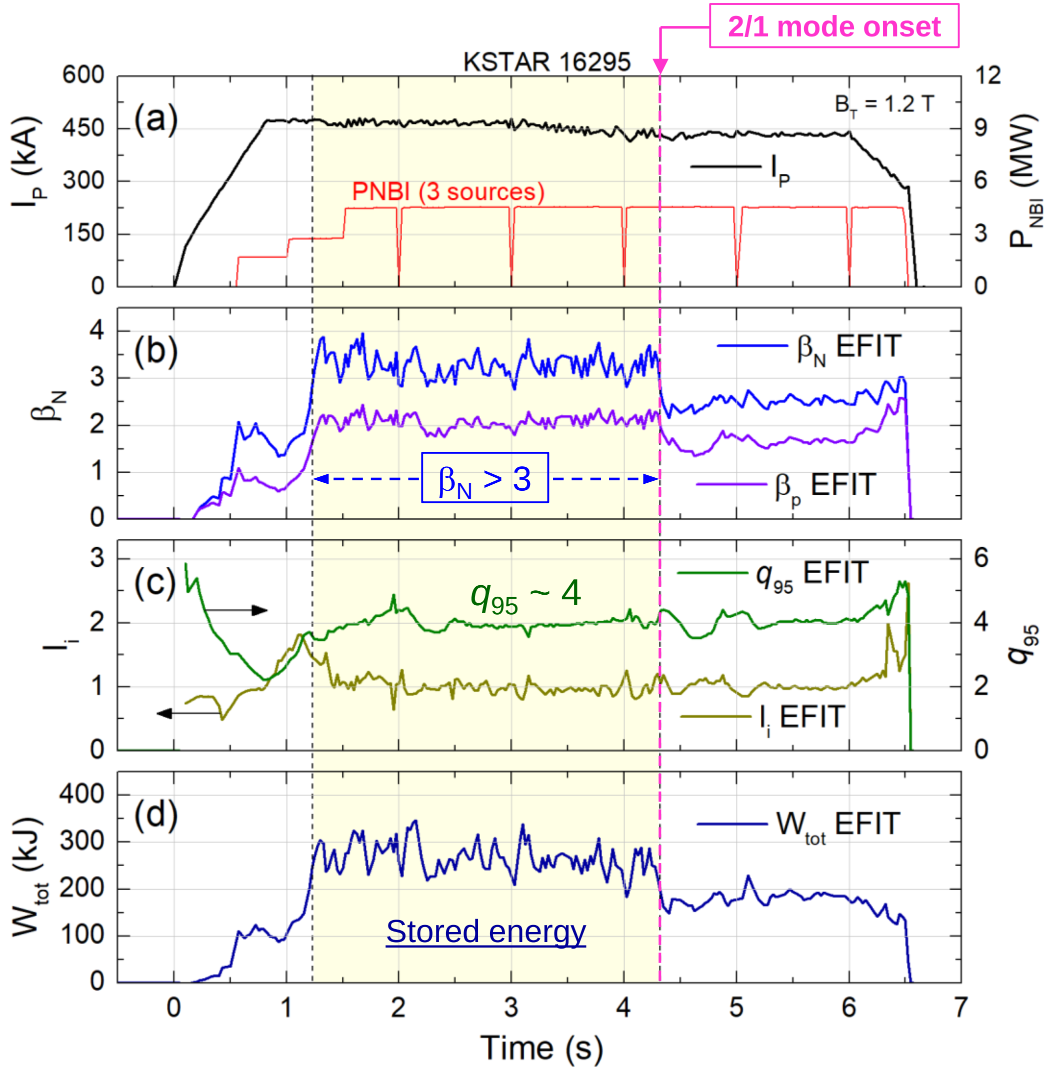

KSTAR high β_N discharge evolution showing parameters from fully converged EFIT reconstructions

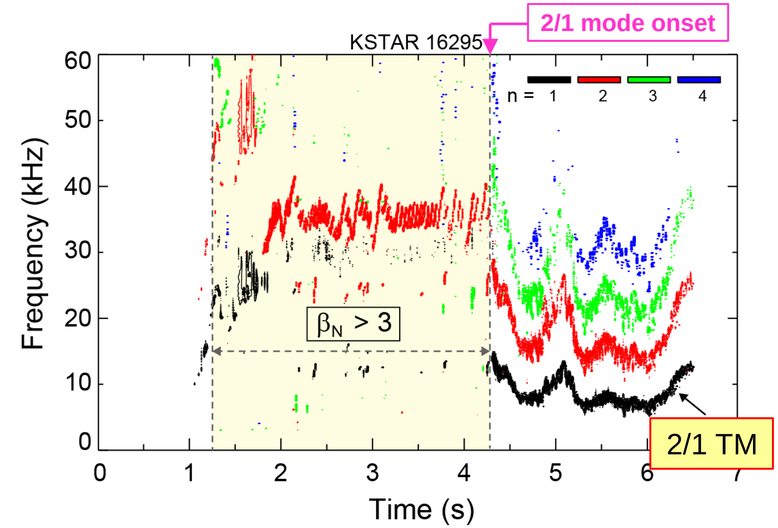

Toroidal magnetic probe spectrum

- Sustained high β_N^{avg} = 3.3 achieved for 3 s
- High β_N operation was limited by strong 2/1 tearing mode onset
  - Measured mode amplitude > 20 G
  - Both W_{tot} and β_N were reduced by ~35% but maintained H-mode
  - The 2/1 mode is expected to be triggered by co-existing sawteeth

Comparative equilibria stable to disruptive MHD instabilities - shot 16325

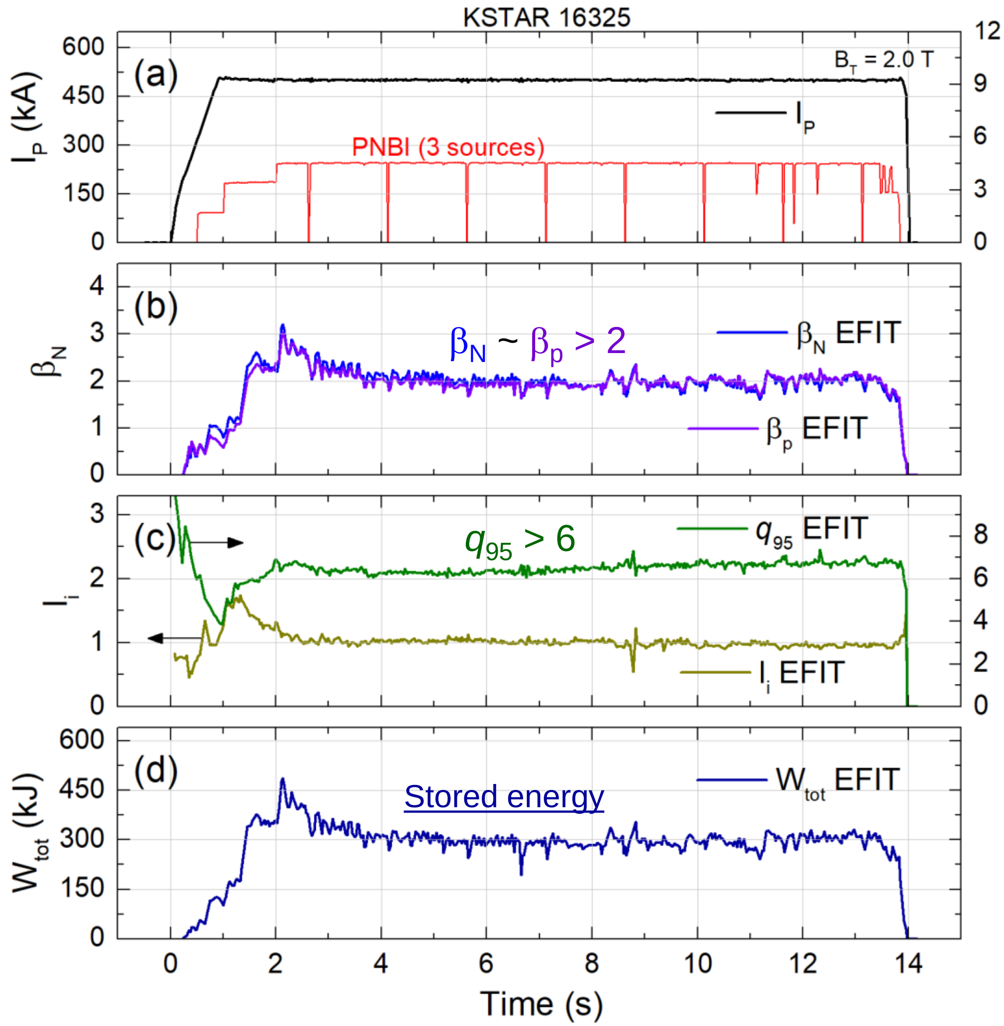

KSTAR 16325 discharge evolution showing parameters from fully converged EFIT reconstructions

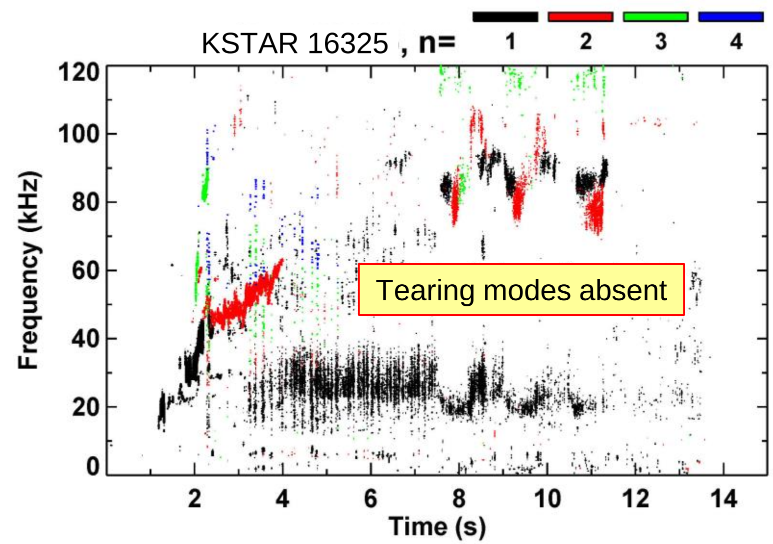

Toroidal magnetic probe spectrum

- Plasma operation at elevated B_T produced equilibria having higher q_{95}
- Unlike shot 16295, discharge doesn't experience any major beta-limiting MHD activities

Kinetic EFIT with MSE constraints used for accurate stability and transport analysis on KSTAR

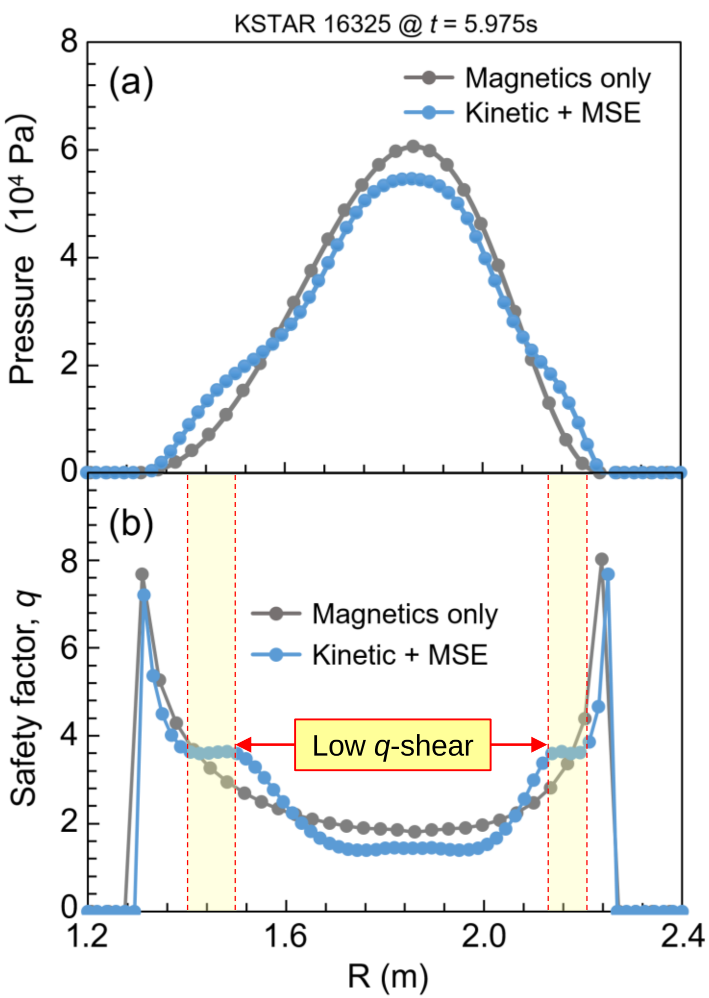

(a) Reconstructed pressure and (b) safety factor profile from kinetic EFIT using internal profile constraints

- Equilibrium reconstruction using measured internal profile constraints provides reliable pressure profile and internal magnetic geometry

  S.A. Sabbagh, Nucl. Fusion **41** (2001) 1601

- KSTAR is equipped with key internal profile diagnostics
  - Charge exchange (T_i, V_ϕ) : 32 CHs
  - Thomson scattering (T_e, n_e) : 27 CHs
  - Motional Stark Effect : 25 CHs
- MSE background polychrometer installed in the device will improve the measurement
- Reconstructed *q*-profile shows region of low shear appear at varied *q*-values in different operational regimes due to broadness of bootstrap current profile

Kinetic EFIT reconstruction shows evolution of low-sheared *q*-profile region at varied *q*-values

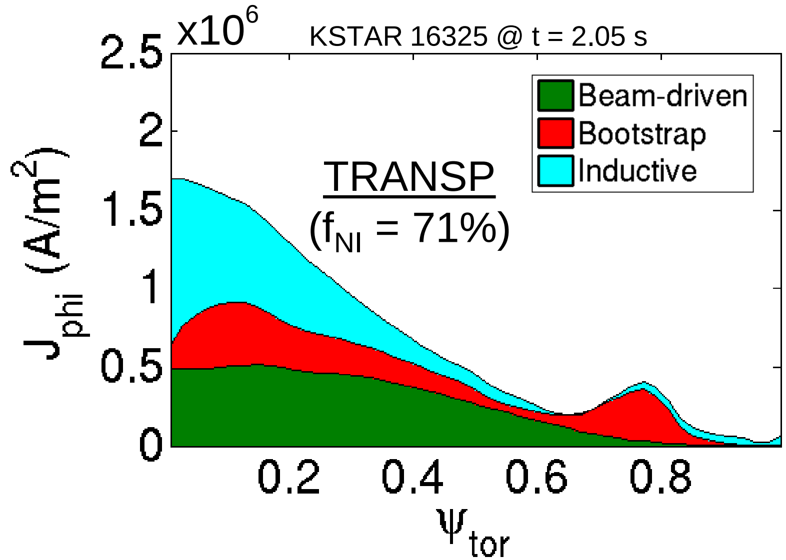

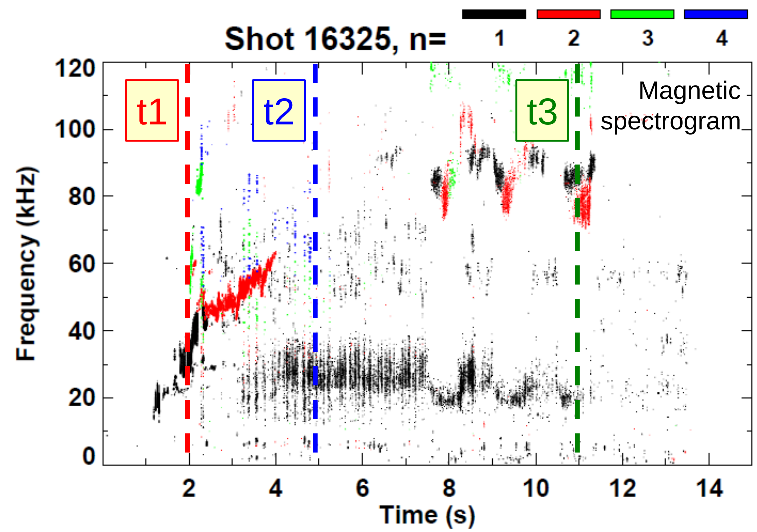

Kinetic + MSE reconstructed *q*-profile evolution

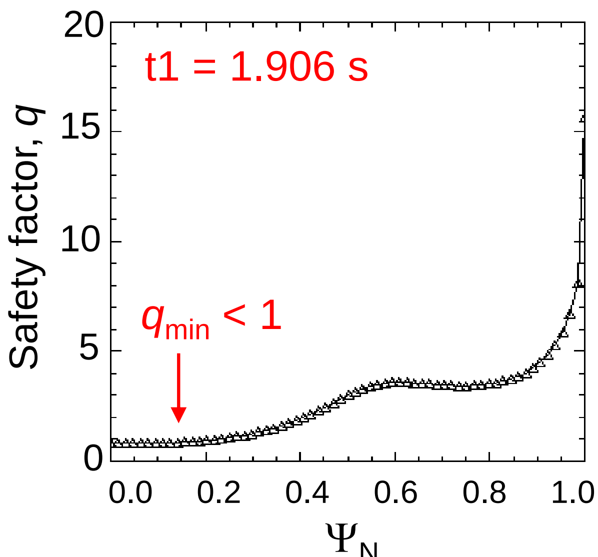

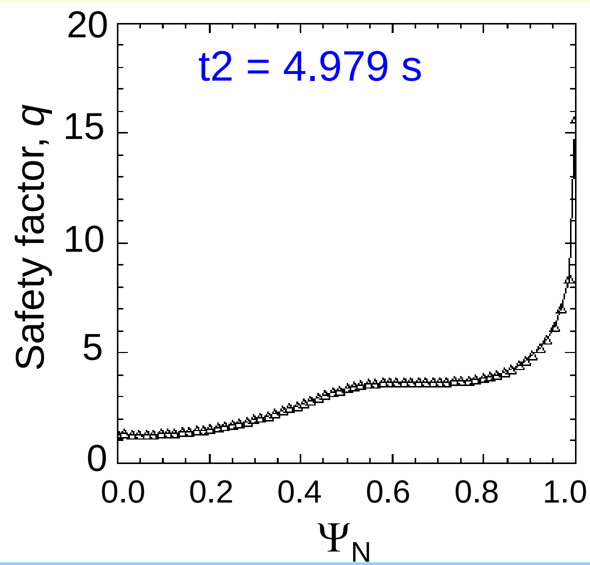

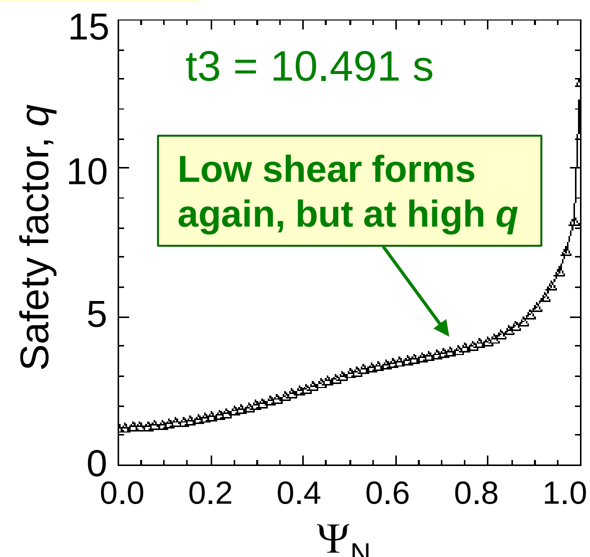

Interpretive TRANSP analysis computes high non-inductive current fraction in the experimental equilibria

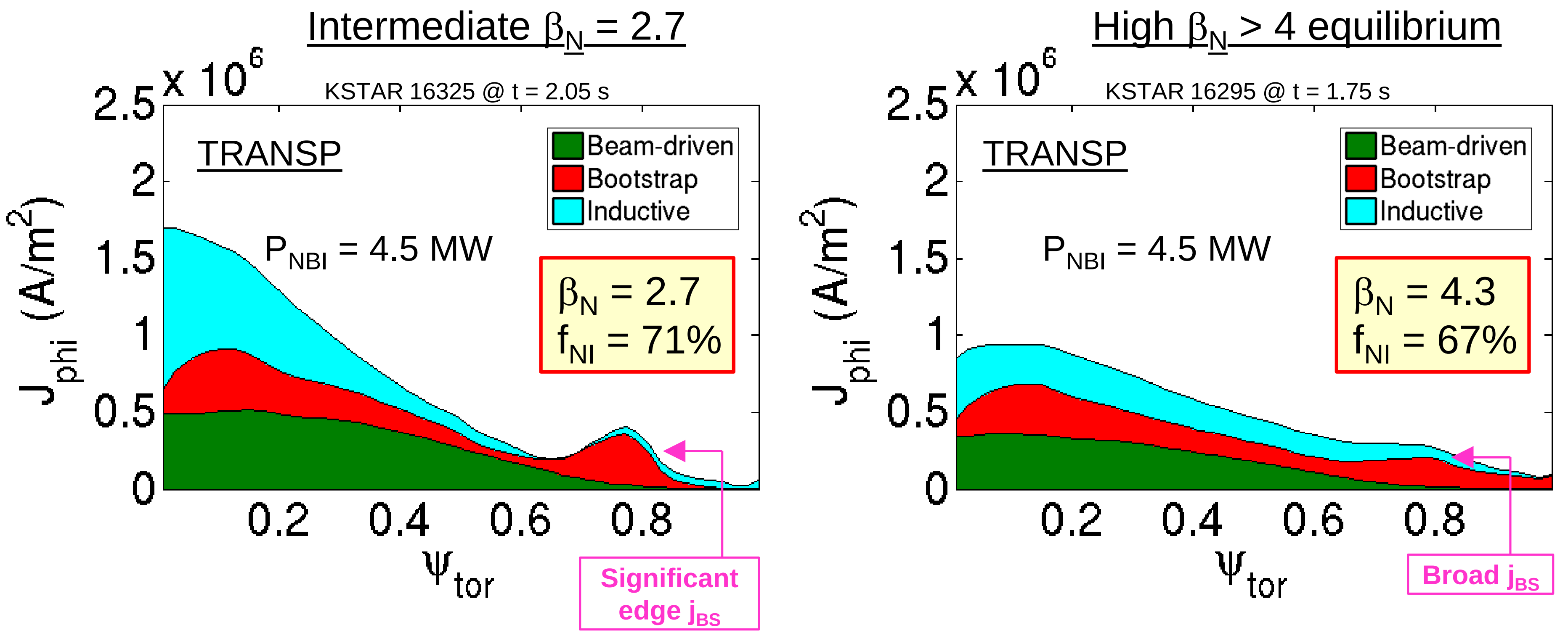

- Transport calculations using TRANSP to investigate a disruption-free path to device target high beta operation with high non-inductive current fraction, f_{NI}
- Interpretive TRANSP runs indicate f_{NI} can reach up to 75% in the experiment
- While f_{NI} can be high in different operating conditions, the bootstrap and total non-inductive current profile can vary significantly

High β_N > 4 can be achieved with near fully non-inductive current by using the planned P_{NBI} increase in KSTAR

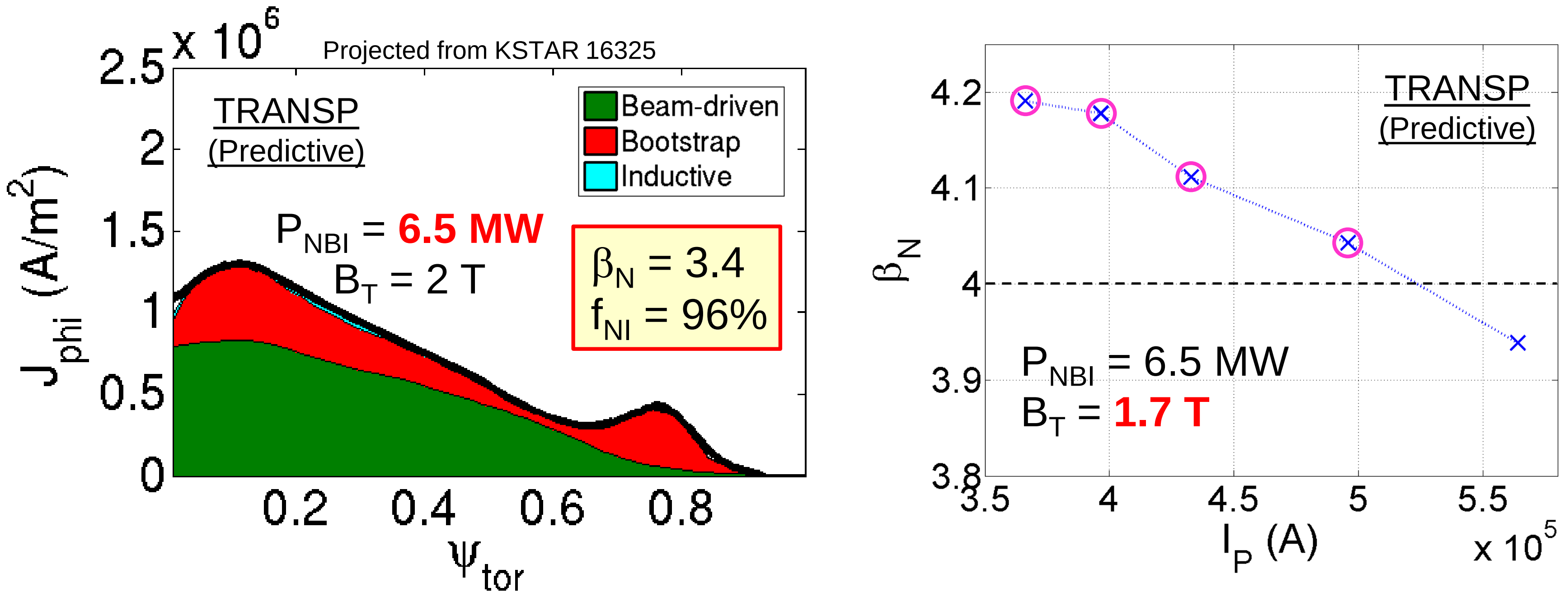

- A new off-axis 2nd NBI system is being installed for the 2018 device operation
- Experimental f_{GW} = 0.5 and H_{98y2} = 1.25 are maintained, and total P_{NBI} = 6.5 MW (P_{NBI-1} = 5 MW, P_{NBI-2} = 1.5 MW) is used in the predictive TRANSP runs
- Predictive runs indicate β_N > 4 can be achieved with fully non-inductive current by using a fraction of the planned P_{NBI} increase (P_{NBI} > 11 MW from 2019)

DCON stability calculation shows high β_N equilibria are subject to n = 1 ideal instability

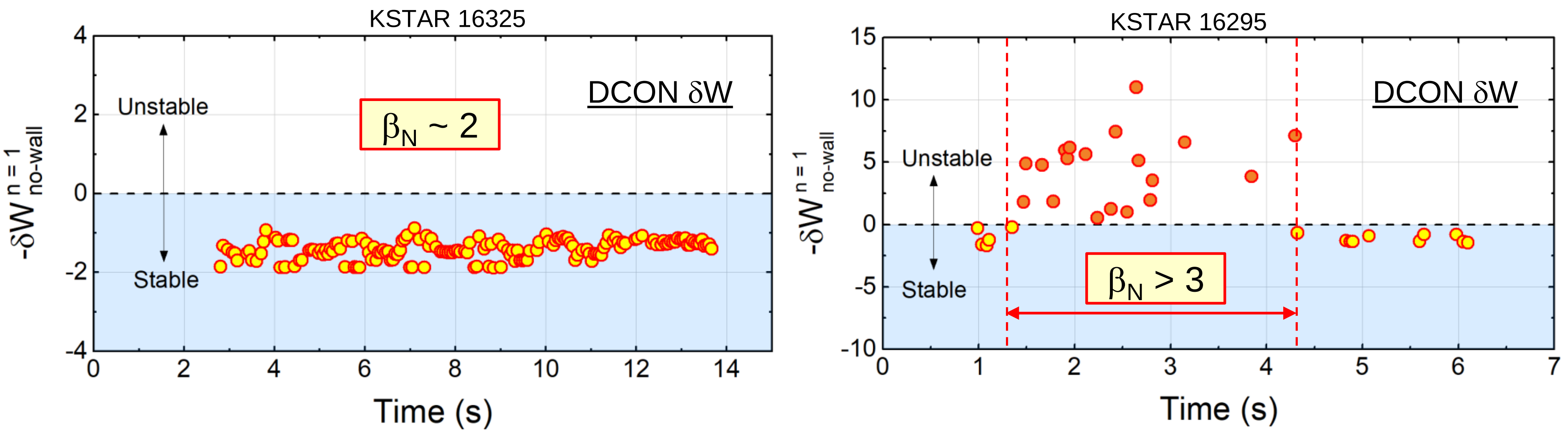

DCON computed ideal MHD n = 1 δW with no-wall

- Equilibria at lower β_N ~ 2 is consistently stable to n = 1 ideal modes in DCON
- Unlike the lower β_N case, DCON calculates unstable n = 1 mode with no-wall ($\beta_N > \beta_N^{no\text{-}wall}$) at the achieved high $\beta_N > 3$
- The small deviations in the reconstructed profiles in the high β_N phase is responsible for reduced equilibrium convergence and the scatter in δW

A.H. Glasser, Phys. Plasmas **23** (2016) 072505

Tearing stability is examined by the resistive DCON code

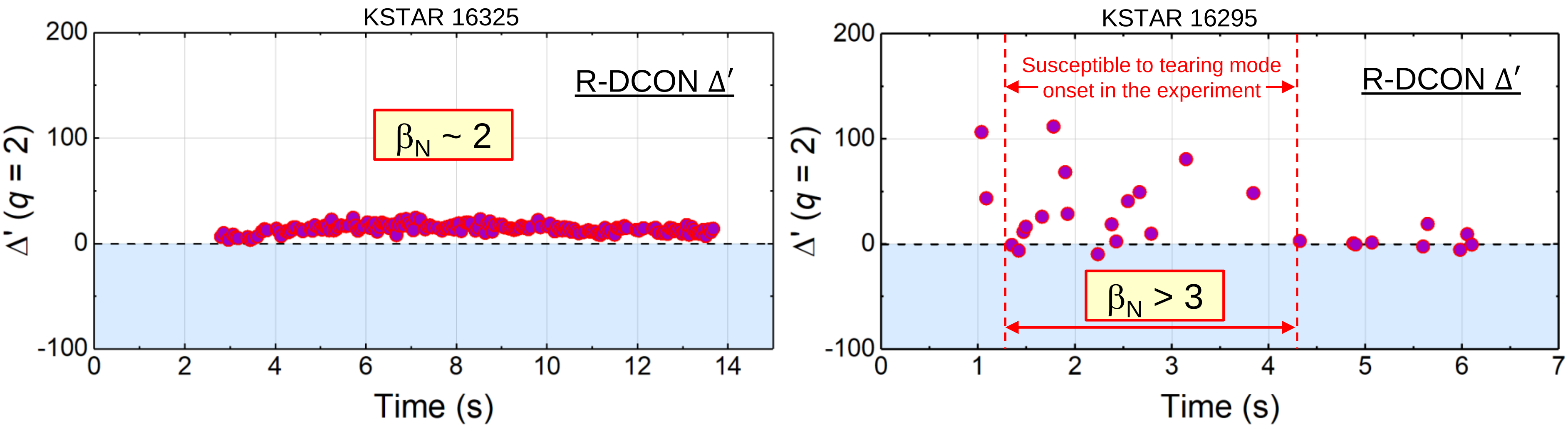

Resistive DCON computed Δ' at q = 2 surface

- The tearing stability index, Δ', at high $\beta_N > 3$ is more unstable compared to that at reduced β_N later in the discharge
- The intermediate $\beta_N \sim 2$ equilibria that are experimentally stable to tearing modes but show an unstable value of Δ' indicate that stabilizing components of the NTM stability combined with sheared toroidal rotation need to be invoked

A.H. Glasser, *et al*., Phys. Plasmas **23** (2016) 112506

Ideal and resistive stability of high β_N equilibria examined by using M3D-C[1]

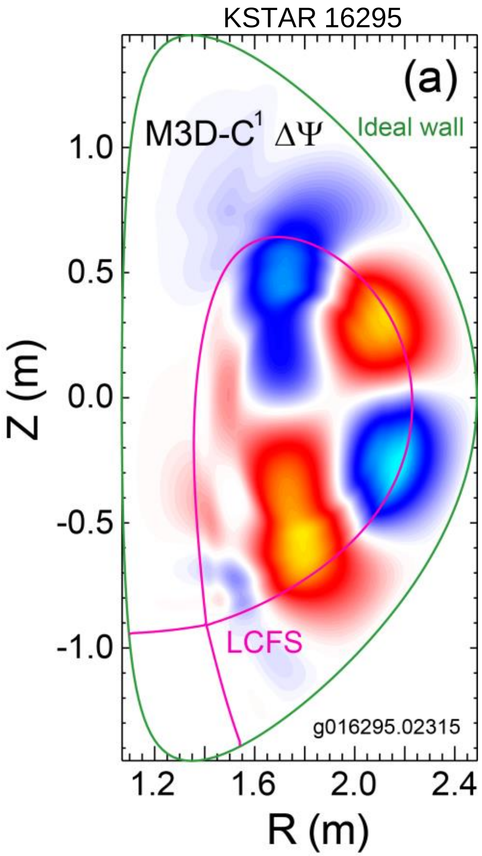

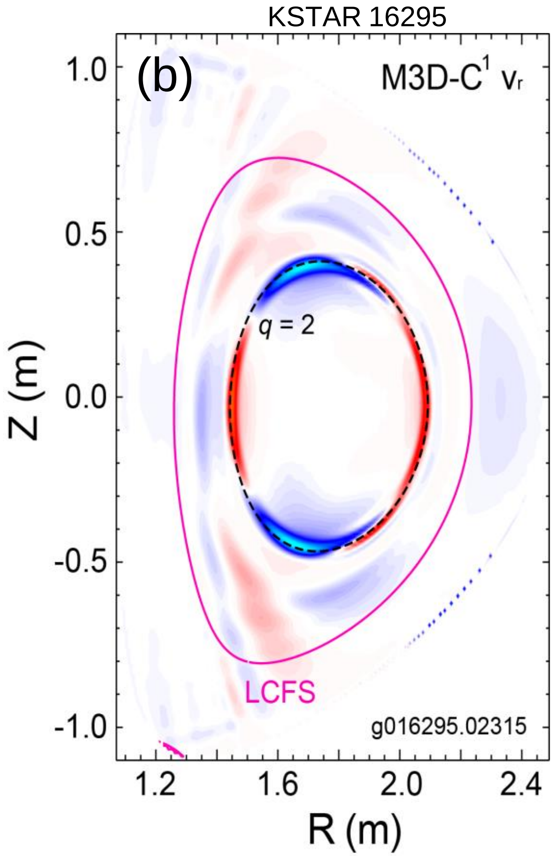

- The high β_N equilibrium is computed to be unstable to n = 1 ideal mode by linear M3D-C[1] analysis consistent with DCON
- Kinetic RWM stability can explain the observed RWM stable operation at $\beta_N > \beta_N^{no\text{-}wall}$
- A marginally stable 2/1 tearing mode is computed in M3D-C[1] using a simplified input plasma resistivity estimated from measured T_e profile

<u>(a) The perturbed poloidal flux of unstable ideal mode and (b) the radial velocity eigenfunction of a 2/1 tearing mode from M3D-C[1]</u>

S.C. Jardin, *et al*., J. Comput. Phys. **226** (2007) 2146

Kinetic modification of RWM stability is evaluated with including energetic particle effects

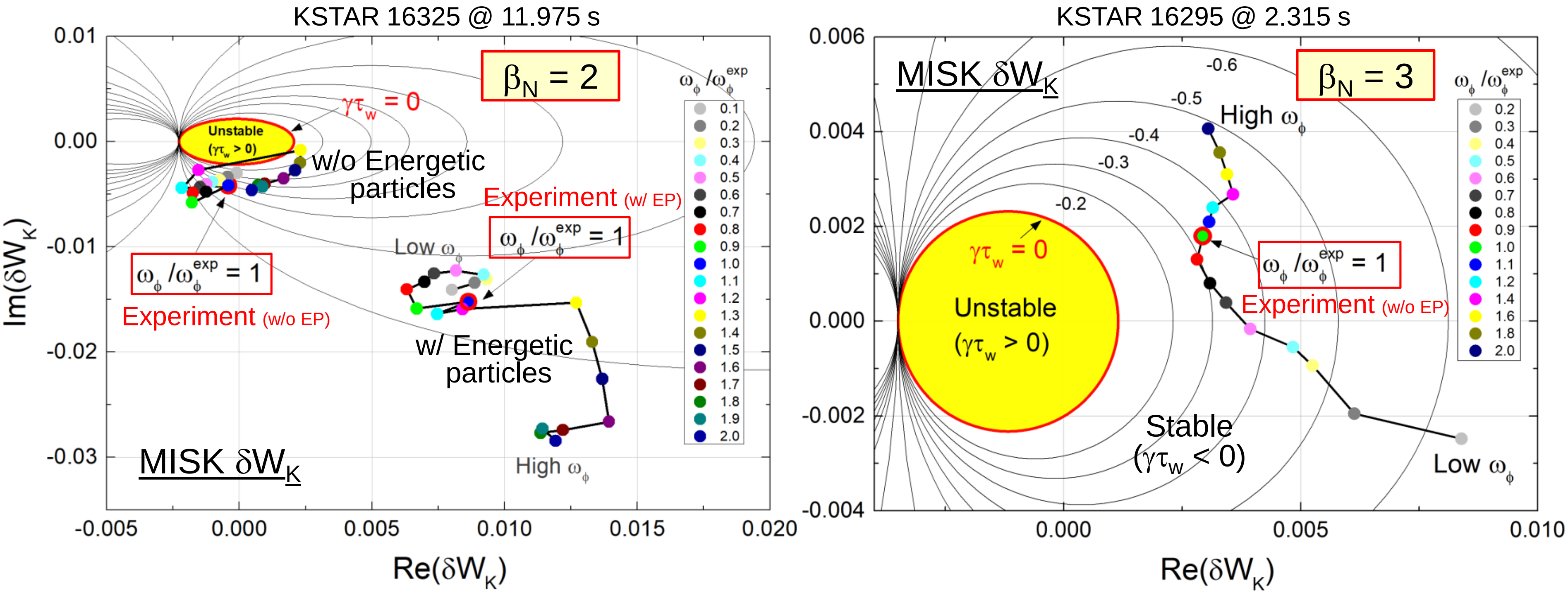

n = 1 RWM stability diagram with scaled experimental rotation profiles

- MISK calculations find the equilibrium is stable to RWM as is consistent with experiment (rotation profile is scaled from 0.1 to 2 times in the analysis)
- Energetic particles are predicted to give a strong stabilizing effect to RWMs

J.W. Berkery, *et al*., PRL **104** (2010) 035003
Y.S. Park, *et al*., Nucl. Fusion **51** (2011) 053001

RWM active feedback control system installed in KSTAR

KSTAR RWM feedback physics model in VALEN-3D

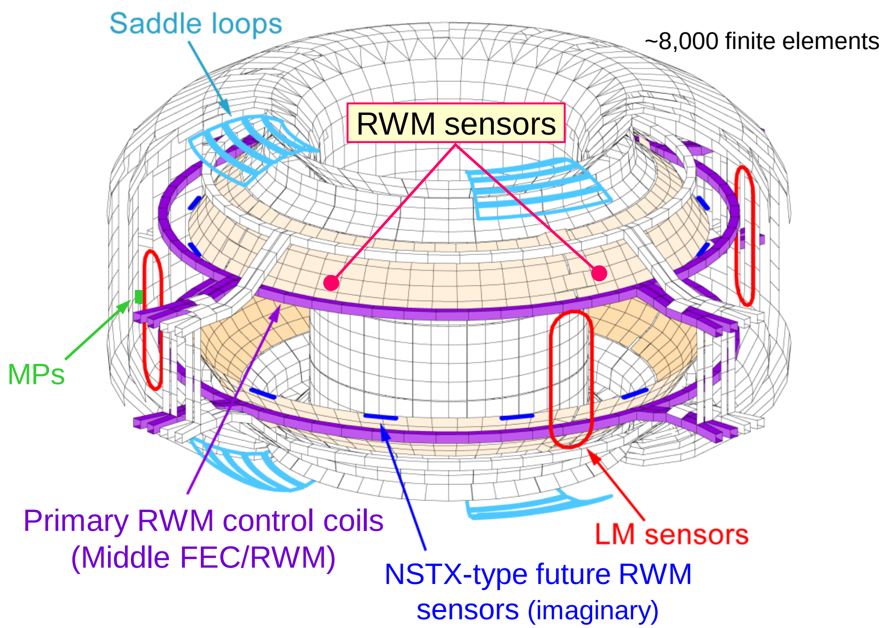

Y.S. Park, *et al*., Phys. Plasmas 21 (2014) 012513

RWM feedback sensors on passive plates

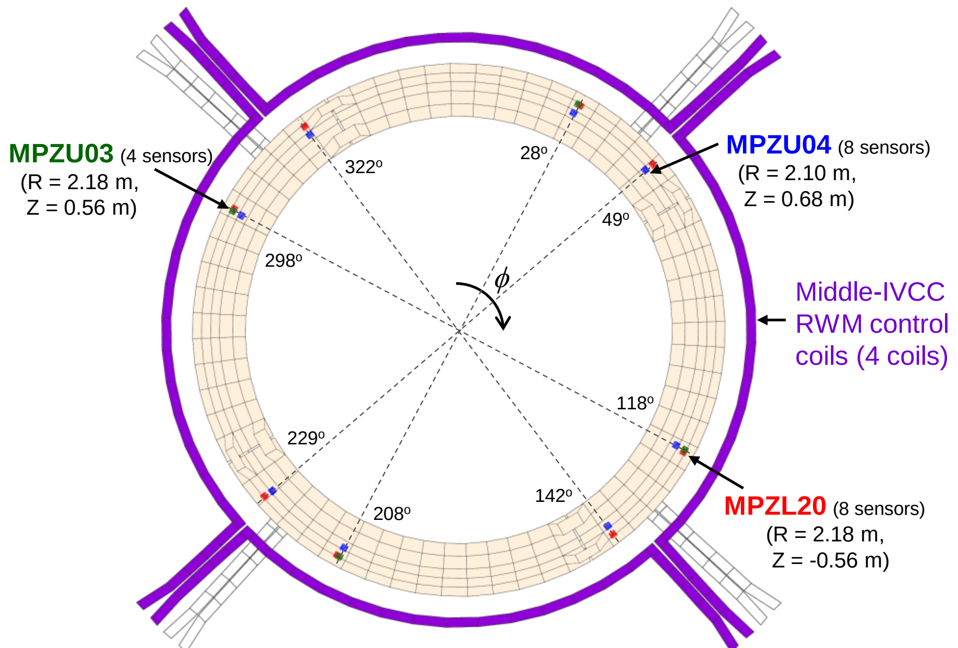

<lower passive plate - top view>

- For plasma operation at $\beta_N > \beta_N^{\text{no-wall}}$, RWM control system is prepared in KSTAR
  - The middle in-vessel control coils (IVCCs) minimizes the inductive shielding by the copper passive stabilizing plates during RWM feedback
  - Three sets of RWM B_p sensors at 8 toroidal positions above and below the midplane have been installed at the inside of the passive plates ⇒ total 20 independent B_p measurements for RWM identification (f_{sample} = 20 kHz)

Magnetic fields from induced currents are compensated from sensor measurement for accurate RWM identification

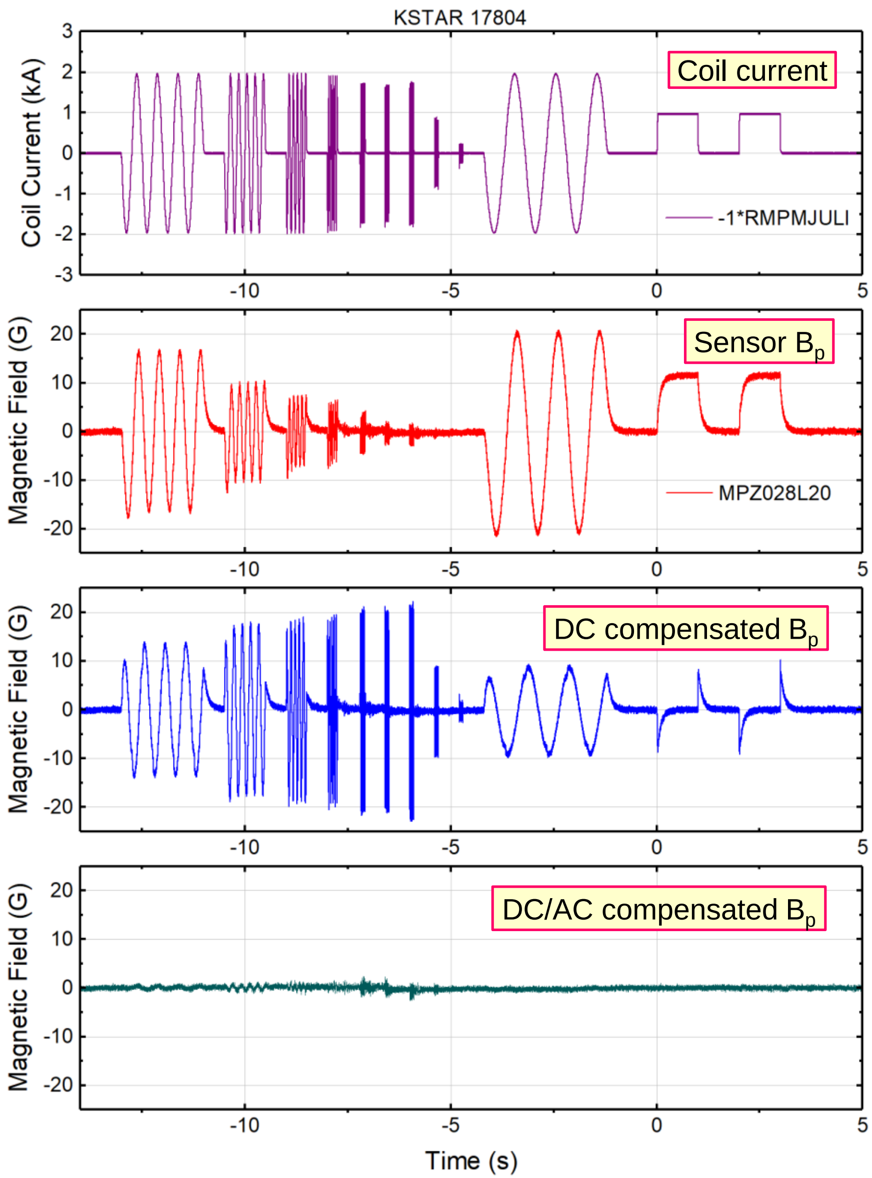

- Define the DC-compensated δB:

$$\delta B_{\mathrm{DC}} = \delta B - \sum_{j}^{N_{\mathrm{coil}}} M_j I_j$$

- Significant inductive component still remains in δB_{DC} due to high sensor mutual coupling to the passive plates
- Similar to NSTX, use low-pass-filtered (LPF) RWM coil current derivative as the source of the inductive δB
- Define the AC-compensated δB:

$$\delta B_{\mathrm{AC}} = \delta B_{\mathrm{DC}} - \sum_{j}^{N_{\mathrm{coil}}} \sum_{k}^{N_\tau} p_{j,k} LPF\left(\frac{dI_{RWM,j}}{dt}; \tau_{AC,k}\right)$$

- Tested three τ_{AC} values well compensates the inductive effect with remaining $|\delta B| <$ 2 G after applying DC/AC compensations

Utilization of multiple RWM sensor arrays is enabled by examining the phase of the perturbed δB of RWMs

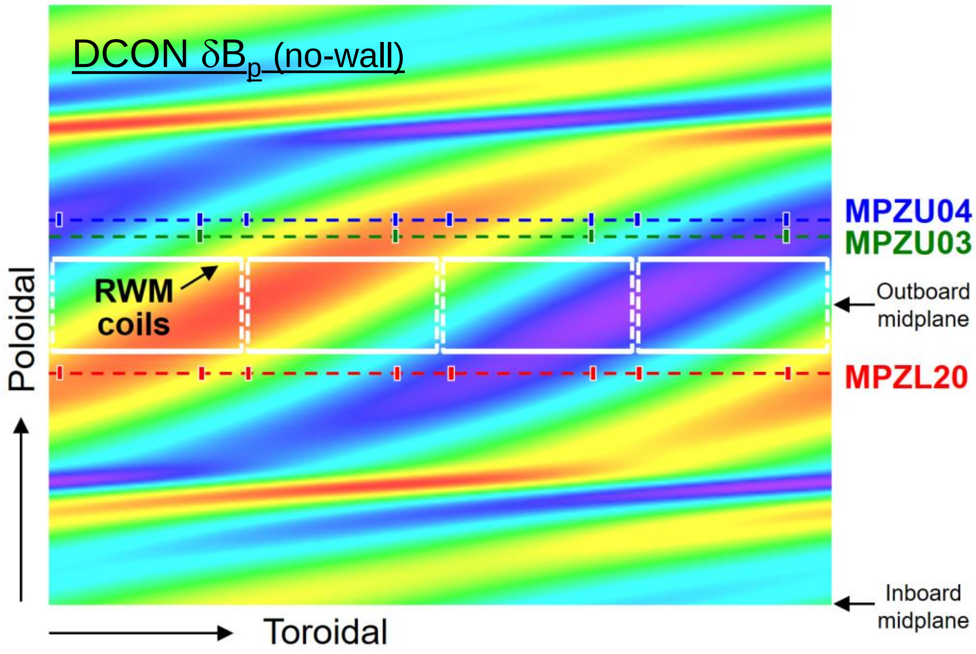

The perturbed δB_p for an unstable n = 1 eigenfunction

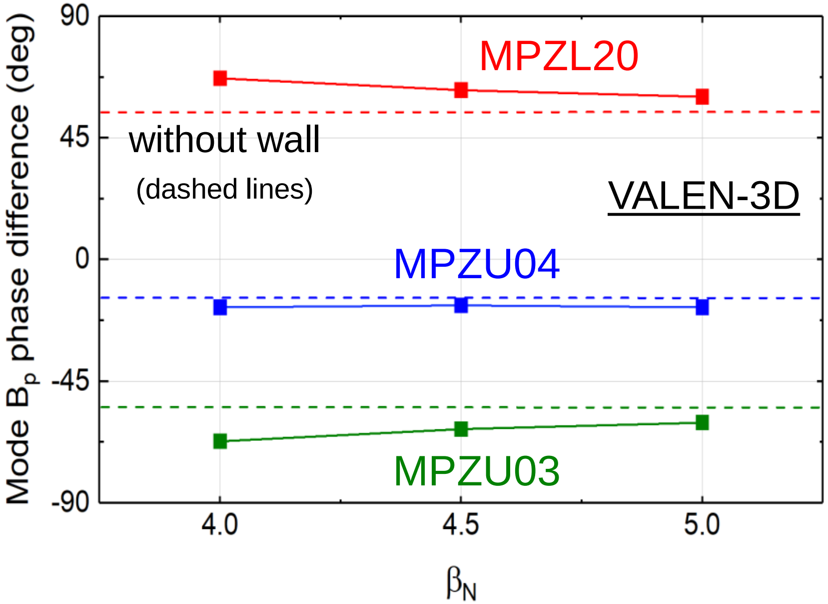

Relative phase of RWM measured by the sensor arrays w.r.t the phase at the midplane

- Utilization of the entire available sensor arrays is beneficial for a better control since the RWM eigenfunction can have varying helicities of δB in the outboard
- The phase difference between the midplane and off-midplane region changes with β_N as the response of the wall increases with faster mode growth
- Assumed sensor toroidal angles in mode decomposition are modified accordingly

Measured amplitude and phase of slowly rotating MHD mode

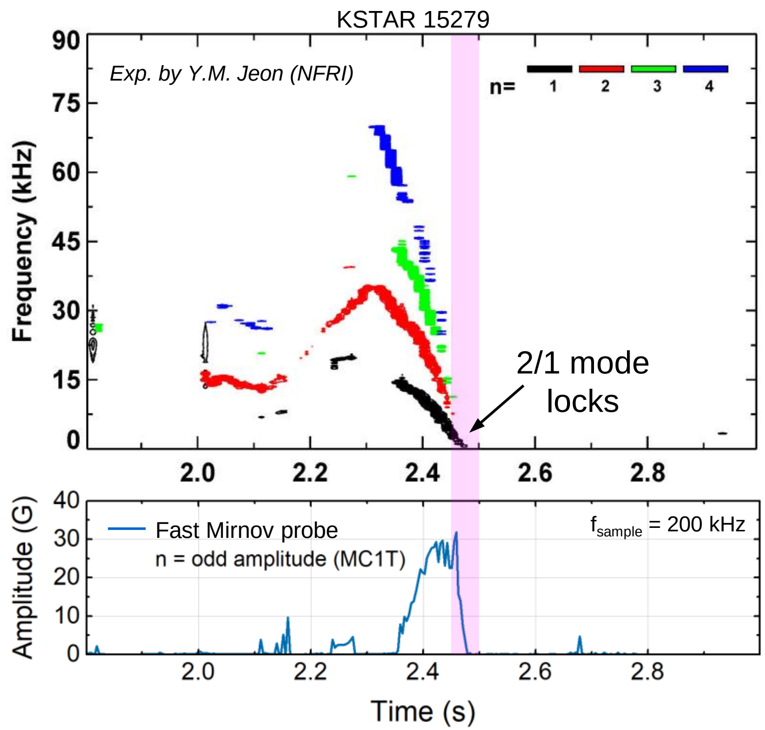

Toroidal magnetic probe spectrum and mode amplitude

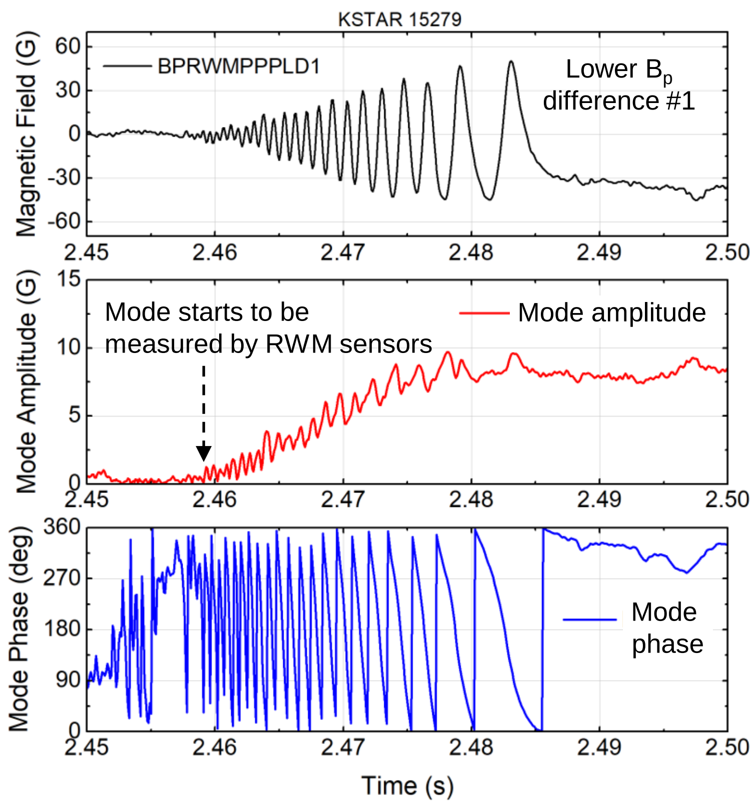

Measured mode amplitude and phase

- Since RWMs have yet to be measured on KSTAR, mode identification has been tested for slowly rotating tearing modes (w/o applied feedback)
- Used 10 B_p sensor differences (180º opposing sensor pairs) for n = 1 identification
- Mode identification well measures the evolution of n = 1 locking tearing mode

Conclusions and Next Steps

- Stability and transport of high performance KSTAR plasmas are analyzed
  - Kinetic EFIT with MSE is used for accurate stability and transport analysis
  - TRANSP analysis computes high $\beta_N > 4$ with fully non-inductive current can be achieved with newly increased P_{NBI} in KSTAR
  - Achieved high β_N equilibria are subject to ideal n = 1 instability (DCON, M3D-C[1])
  - Resistive DCON analysis emphasizes the role of the pressure driven effects in the observed tearing stability
  - MISK analysis can explain the observed RWM stable operation at high $\beta_N > \beta_N^{no\text{-}wall}$
- Development of algorithm for RWM identification and feedback
  - Significant δB produced by induced currents in conducting structures is compensated from RWM sensors, and utilization of multiple sensor arrays is enabled by examining the perturbed δB structure of RWMs
- Next Steps
  - Improve stability analysis by employing the pressure driven terms of NTM stability
  - Test the developed RWM feedback algorithm in high β_N experiment
  - Experiments are scheduled in 2018 to improve sustained high β_N, and probe stability

BACKUP SLIDES

Onset of strong 2/1 tearing mode terminated high β_N

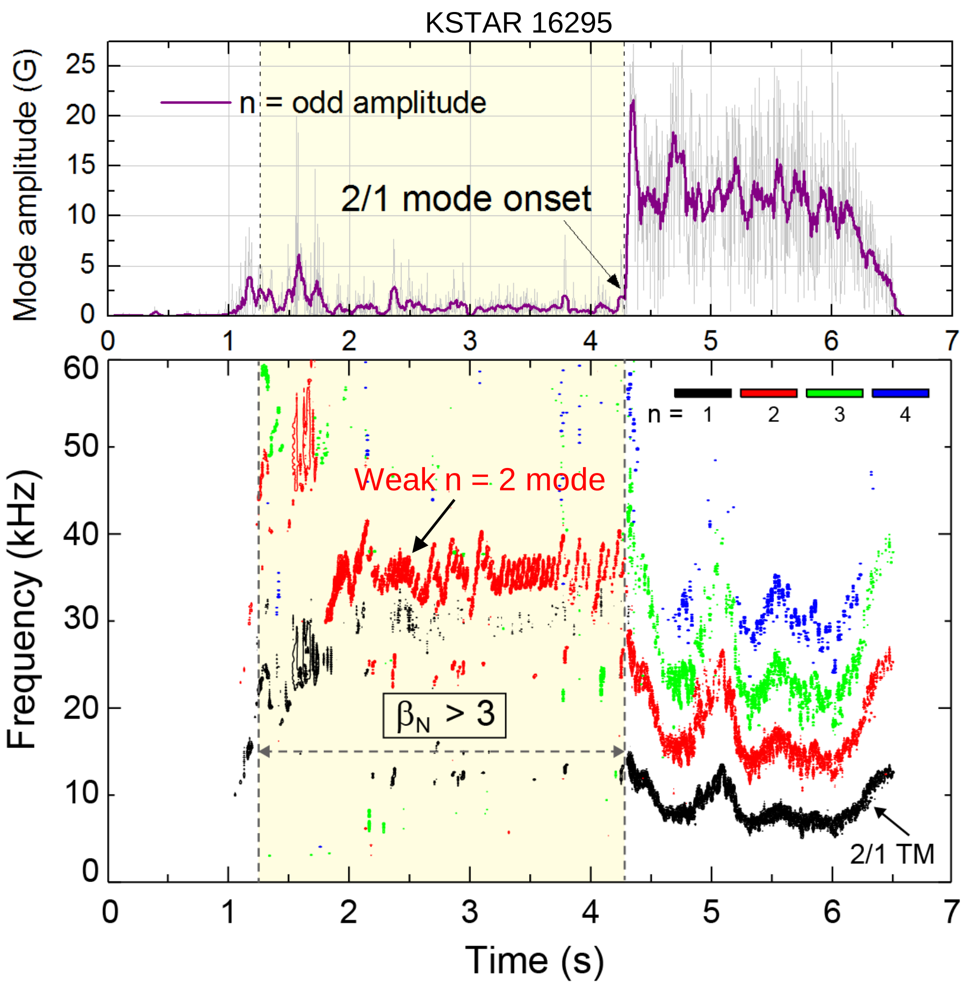

Toroidal magnetic probe spectrum and mode amplitude in high β_N discharge

- At high β_N phase, a benign n = 2 mode (presumably 3/2 mode) exists with strong sawteeth
  - No indication of W_{tot} reduction due to the n = 2 mode having $|\tilde{B}_p|$ ~ 2 G
- High β_N operation was limited by strong 2/1 tearing mode onset
  - Measured mode amplitude > 20 G
  - Both W_{tot} and β_N were reduced by ~35% but maintained H-mode
  - Similar discharges exhibited different 2/1 tearing mode onset time (expected to be triggered by sawteeth)
- Plasma rotation profile significantly reduced by > 20% due to the 2/1 mode onset

RWM stability evaluated with ideal and kinetic components allows for passive stabilization of the RWM

- Kinetic effects modify ideal MHD n = 1 stability (MISK code)
  - Collisional dissipation
  - Rotational stabilization

kinetic modification

$$(\gamma - i\omega_r)\tau_w = -\frac{\delta W_\infty + \boxed{\delta W_K}}{\delta W_b + \boxed{\delta W_K}}$$

B. Hu, *et al*., PRL **93** (2004) 105002
J.W. Berkery, *et al*., PRL **104** (2010) 035003
S.A. Sabbagh, *et al*., Nucl. Fusion **50** (2010) 025020

<u>Trapped ion component (typically dominates Re(δW_K))</u>

$$\delta W_K \propto \int \left[\frac{\omega_{*N} + \left(\hat{\varepsilon} - \frac{3}{2}\right)\omega_{*T} + \omega_E - \omega - i\gamma}{\underbrace{\langle \omega_D \rangle}_{\text{precession drift}} + \underbrace{l\omega_b}_{\text{bounce}} - \underbrace{i\nu_{eff}}_{\text{collisionality}} + \underbrace{\omega_E}_{\text{E}\times\text{B}} - \omega - i\gamma} \right] \hat{\varepsilon}^{\frac{5}{2}} e^{-\hat{\varepsilon}} d\hat{\varepsilon}$$

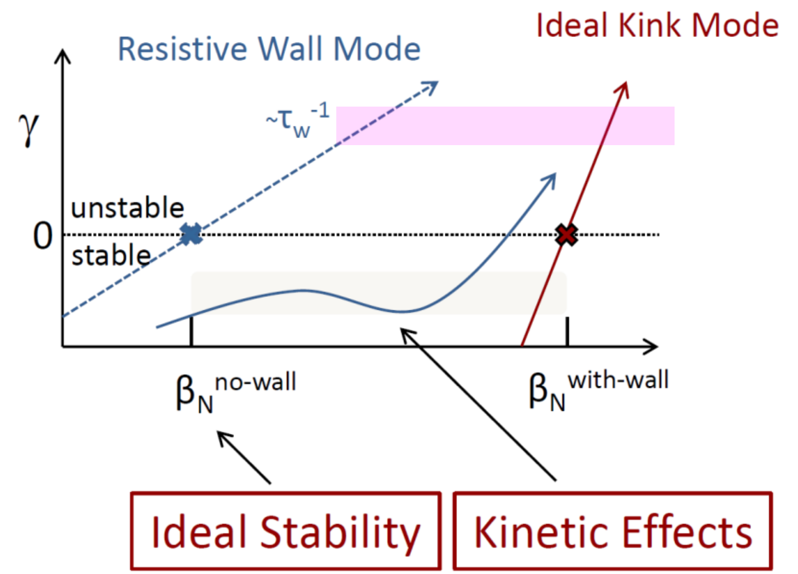

J.W. Berkery, *et al*., MHD Workshop (2015)

- Stability modification depends on
  - Integrated ω_ϕ profile: resonances in δW_K
  - Particle collisionality

- Plasma is stable when rotation is in resonance
  - l = 0 harmonic : resonance with precession drift frequency $\boxed{\omega_E + \langle \omega_D \rangle = 0}$
  - l = -1 harmonic : resonance with bounce frequency $\boxed{\omega_E + \langle \omega_D \rangle - \omega_b = 0}$

New RWM sensors will give superior control performance over the previous device sensors

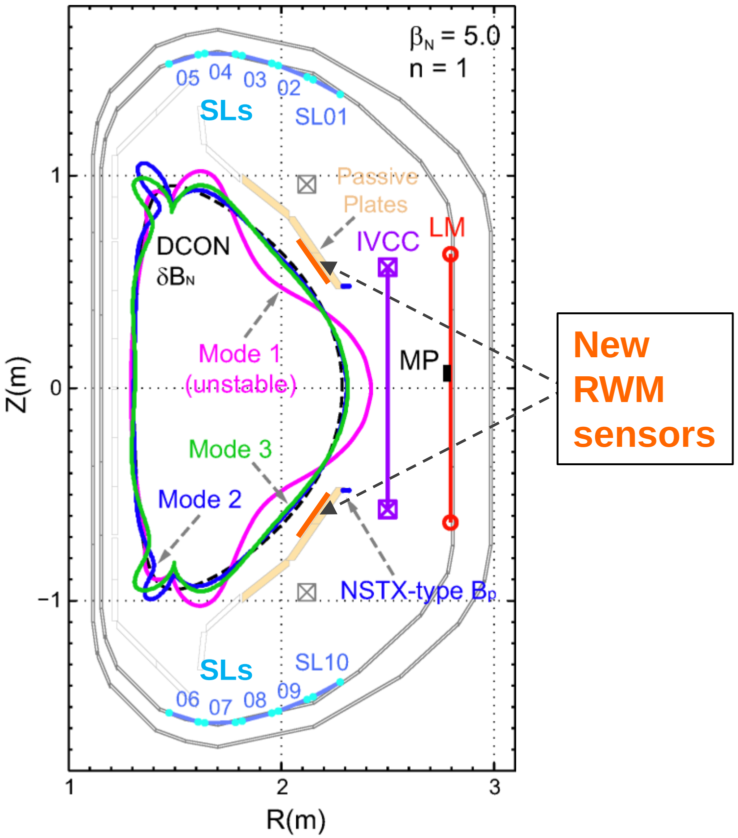

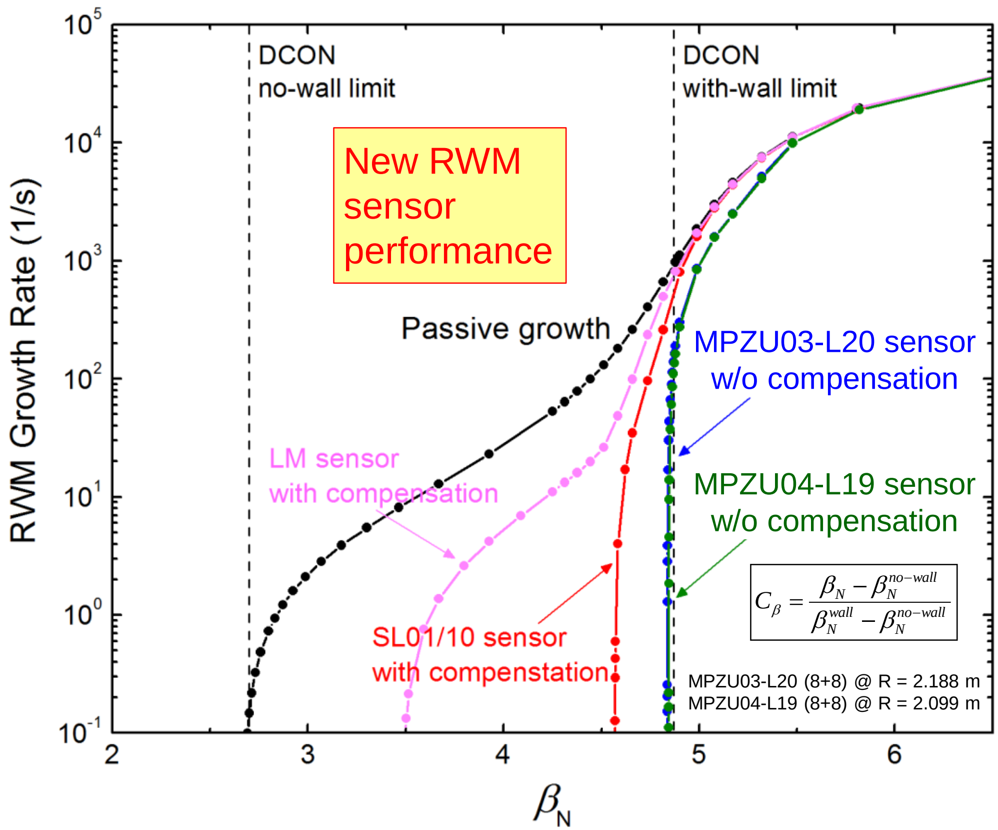

Y.S. Park, *et al*., Phys. Plasmas **21** (2014) 012513

RWM control performance of the new RWM sensors

- The design advantages of the new RWM sensors result in greater mode control - almost up to the ideal with-wall limit (C_β = 98%, β_N = 4.8)

Strong coupling between RWM feedback sensors and passive plates could be detrimental to RWM feedback

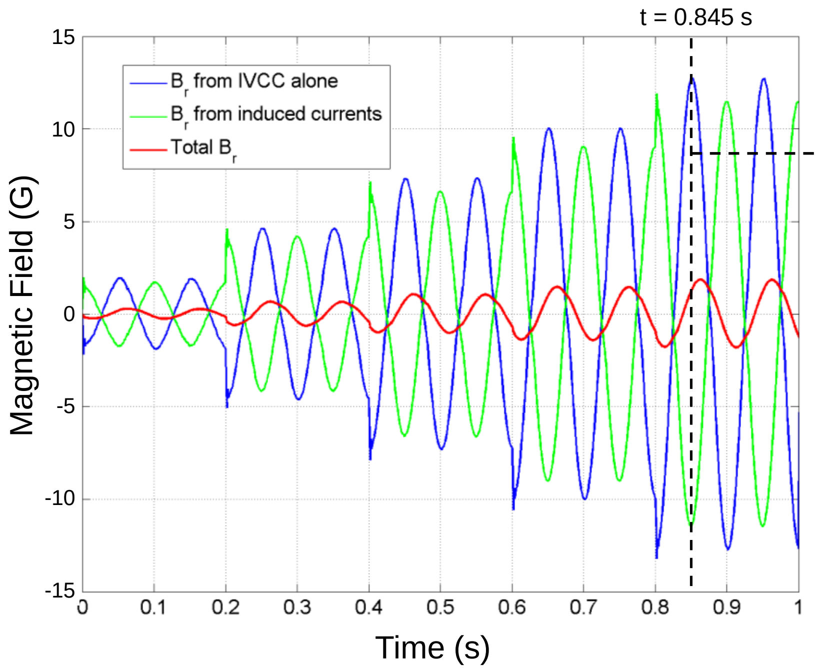

VALEN-3D computed sensor measurement

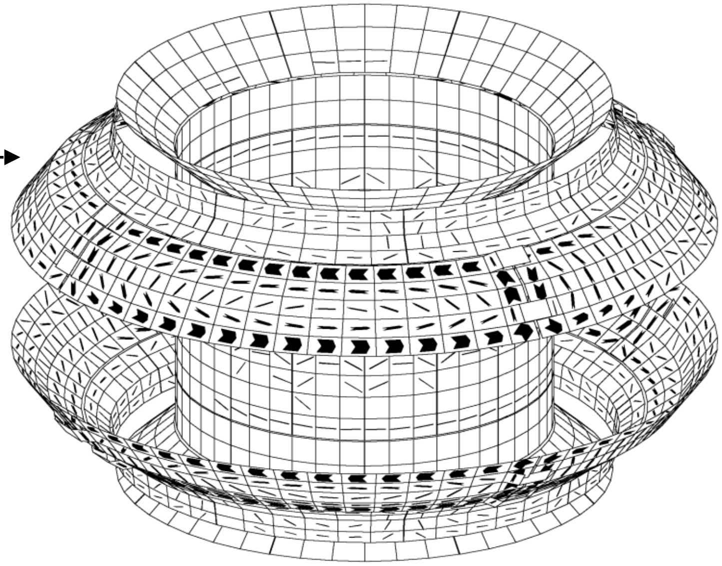

Computed induced currents on the internal passive conductors when 10 Hz n = 1 rotating field is applied from RWM control coils (m-IVCCs)

- Transient effects of the induced currents on the passive plates have been examined by VALEN-3D code
- KSTAR passive plates are found to give a significant inductive effect on RWM sensor measurement when RWM coils are activated

AC sensor compensation can eliminate the remaining δB components after the DC compensations

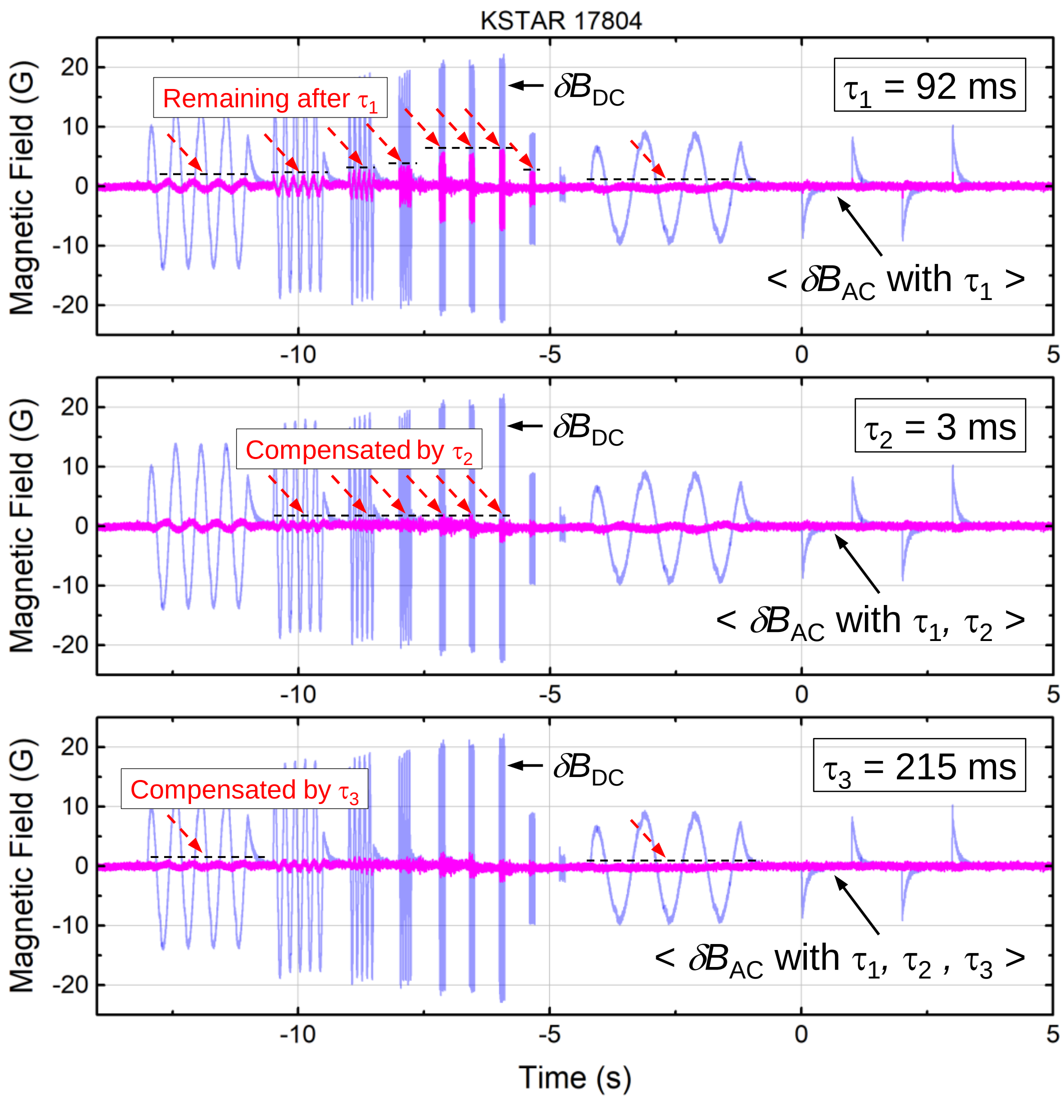

- Similar to NSTX, use low-pass-filtered (LPF) RWM coil currents as the source of the inductive δB
- Define the AC compensated δB:

$$\delta B_{\mathrm{AC}} = \delta B_{\mathrm{DC}} - \sum_{j}^{N_{\mathrm{coil}}} \sum_{k}^{N_{\tau}} p_{j,k} LPF\left(\frac{dI_{RWM,j}}{dt}; \tau_{AC,k}\right)$$

- The coefficient matrix p has max. 20 (N_{sensor}) x 12 (N_{coil}) x 3 (N_{τ}) = 720 elements
- LPF with 3 different τ values has been tested
- Tested τ set well compensates the inductive effect. For the entire RWM sensors, remaining $|\delta B|$ < 2 G after DC+AC compensations

Algorithms for mode identification

- The magnetic perturbation has an amplitude (A_{RWM}) and phase (ϕ_{RWM})

$$B(\phi) = A_{RWM}\cos(\phi - \phi_{RWM})$$

- At the *i*-th sensor, the measured mode amplitude is:

$$B_i = A_{RWM}\cos(\phi_i - \phi_{RWM})$$
$$B_i = A_{RWM}\cos(\phi_{RWM})\cos(\phi_i) + A_{RWM}\sin(\phi_{RWM})\sin(\phi_i)$$
$$B_i = C_{RWM}\cos(\phi_i) + S_{RWM}\sin(\phi_i)$$

- Combine signals to form an amplitude and phase of the plasma 3D perturbation

$$\begin{bmatrix} B_1 \\ B_2 \\ \vdots \\ B_N \end{bmatrix} = \begin{bmatrix} \cos(\phi_1) & \sin(\phi_1) \\ \cos(\phi_2) & \sin(\phi_2) \\ \vdots & \vdots \\ \cos(\phi_N) & \sin(\phi_N) \end{bmatrix} \begin{bmatrix} C_{RWM} \\ S_{RWM} \end{bmatrix} = M \begin{bmatrix} C_{RWM} \\ S_{RWM} \end{bmatrix} \Rightarrow \begin{bmatrix} C_{RWM} \\ S_{RWM} \end{bmatrix} = M^{-1} \begin{bmatrix} B_1 \\ B_1 \\ \vdots \\ B_N \end{bmatrix} \Rightarrow \boxed{\begin{aligned} A_{RWM} &= \sqrt{C_{RWM}^2 + S_{RWM}^2} \\ \phi_{RWM} &= \operatorname{atan}\left(S_{RWM}/C_{RWM}\right) \end{aligned}}$$

M : mode-ID matrix (20 x 2) for KSTAR

- Convert the sensor fields at each time point to amplitude and phase
- Outputs passed within PCS to RWM feedback algorithms for control current request
- Algorithm is presently being implemented in KSTAR PCS for use in 2018